



Contents lists available at ScienceDirect

Acta Biomaterialia

journal homepage: [www.elsevier.com/locate/actabiomat](http://www.elsevier.com/locate/actabiomat)

Full length article

# Mechanically stimulated osteochondral organ culture for evaluation of biomaterials in cartilage repair studies

M.L. Vainieri<sup>a,b</sup>, D. Wahl<sup>a</sup>, M. Alini<sup>a</sup>, G.J.V.M. van Osch<sup>b,c</sup>, S. Grad<sup>a,\*</sup><sup>a</sup> AO Research Institute Davos, Davos Platz, Switzerland<sup>b</sup> Department of Orthopaedics, Erasmus MC, University Medical Centre Rotterdam, The Netherlands<sup>c</sup> Department of Otorhinolaryngology, Head and Neck Surgery, Erasmus MC, University Medical Centre Rotterdam, The Netherlands

## ARTICLE INFO

## Article history:

Received 13 June 2018

Received in revised form 15 August 2018

Accepted 27 September 2018

Available online xxxx

## Keywords:

Articular cartilage

Osteochondral defect

Bioreactor

Ex vivo model

Biomaterials

## ABSTRACT

Surgical procedures such as microfracture or autologous chondrocyte implantation have been used to treat articular cartilage lesions; however, repair often fails in terms of matrix organization and mechanical behaviour. Advanced biomaterials and tissue engineered constructs have been developed to improve cartilage repair; nevertheless, their clinical translation has been hampered by the lack of reliable *in vitro* models suitable for pre-clinical screening of new implants and compounds.

In this study, an osteochondral defect model in a bioreactor that mimics the multi-axial motion of an articulating joint, was developed. Osteochondral explants were obtained from bovine stifle joints, and cartilage defects of 4 mm diameter were created. The explants were used as an interface against a ceramic ball applying dynamic compressive and shear loading. Osteochondral defects were filled with chondrocytes-seeded fibrin-polyurethane constructs and subjected to mechanical stimulation. Cartilage viability, proteoglycan accumulation and gene expression of seeded chondrocytes were compared to free swelling controls. Cells within both cartilage and bone remained viable throughout the 10-day culture period. Loading did not wear the cartilage, as indicated by histological evaluation and glycosaminoglycan release. The gene expression of seeded chondrocytes indicated a chondrogenic response to the mechanical stimulation. Proteoglycan 4 and cartilage oligomeric matrix protein were markedly increased, while mRNA ratios of collagen type II to type I and aggrecan to versican were also enhanced. This mechanically stimulated osteochondral defect culture model provides a viable microenvironment and will be a useful pre-clinical tool to screen new biomaterials and biological regenerative therapies under relevant complex mechanical stimuli.

## Statement of Significance

Articular cartilage lesions have a poor healing capacity and reflect one of the most challenging problems in orthopedic clinical practice. The aim of current research is to develop a testing system to assess biomaterials for implants, that can permanently replace damaged cartilage with the original hyaline structure and can withstand the mechanical forces long term.

Here, we present an osteochondral *ex vivo* culture model within a cartilage bioreactor, which mimics the complex motion of an articulating joint *in vivo*. The implementation of mechanical forces is essential for pre-clinical testing of novel technologies in the field of cartilage repair, biomaterial engineering and regenerative medicine. Our model provides a unique opportunity to investigate healing of articular cartilage defects in a physiological joint-like environment.

© 2018 Acta Materialia Inc. Published by Elsevier Ltd. This is an open access article under the CC BY-NC-ND license (<http://creativecommons.org/licenses/by-nc-nd/4.0/>).

## 1. Introduction

Articular cartilage is a unique tissue, allowing low-friction movement of an articulating joint and withstanding considerable stress and repeated loading, thereby preserving the joint homeostasis. Damage of articular cartilage is prone to progression into

\* Corresponding author at: AO Research Institute Davos, Clavadelerstrasse 8, 7270 Davos Platz, Switzerland.

E-mail addresses: [letizia.vainieri@aofoundation.org](mailto:letizia.vainieri@aofoundation.org) (M.L. Vainieri), [dieter.wahl@aofoundation.org](mailto:dieter.wahl@aofoundation.org) (D. Wahl), [mauro.alini@aofoundation.org](mailto:mauro.alini@aofoundation.org) (M. Alini), [g.vanosch@erasmusmc.nl](mailto:g.vanosch@erasmusmc.nl) (G.J.V.M. van Osch), [sibylle.grad@aofoundation.org](mailto:sibylle.grad@aofoundation.org) (S. Grad).

<https://doi.org/10.1016/j.actbio.2018.09.058>

1742-7061/© 2018 Acta Materialia Inc. Published by Elsevier Ltd.

This is an open access article under the CC BY-NC-ND license (<http://creativecommons.org/licenses/by-nc-nd/4.0/>).

early osteoarthritis (OA); due to the limited repair ability, surgical procedures are required to treat cartilage lesions [1,2]. The two most common approaches to regenerate neocartilage *in situ*, microfracture and autologous chondrocytes implantation (ACI), are well-established procedures for such defects [3–8]. However, cartilage repair outcome after microfracture faces high inter-patient variability [9,10]. In most cases, little or no hyaline cartilage is regenerated, and the generated hyaline cartilage may turn into a weaker fibrocartilage unable to withstand the compression and shear forces [11–13]. On the other hand, the ACI procedure implies multiple surgeries and requires long recovery time; moreover, the chondrocytes dedifferentiate during *in vitro* expansion and their decreased number and activity with aging may impair the healing or result in failure of repair [14,15]. Improved understanding about the mechanisms that are involved in the formation of repair tissue is needed to further develop these procedures.

Current research aims to improve the biological and functional outcome of cartilage repair treatments; for example, functional cartilage tissue engineering aims to generate neo-tissue *in situ* with an articular surface similar to that of native cartilage [16]. For *ex vivo* investigations, the use of bioreactors has been introduced to mimic the multi-axial motion of an articulating joint and reproduce the kinematics of mechanical loading experienced by chondrocytes *in vivo* [17]. It has been reported that cyclic compression combined with shear stresses act as modulators of the amount and type of extracellular matrix (ECM) synthesized [18], as promoters of functional articular surfaces [19,20], and as an inducer of transforming growth factor-beta (TGF- $\beta$ 1) production and activation, thereby promoting chondrogenesis of mesenchymal stem cells [21–24]. Therefore, implementation of mechanical forces is essential for the development and maintenance of articular cartilage and is required for more predictive pre-clinical *ex vivo* research.

Osteochondral *ex vivo* models [25] in which chondral or osteochondral defects can be generated, are of great value for translational research. In contrast to cell culture models, the osteochondral explant culture model allows investigations of the interplay between cellular and extracellular signals involved in cartilage repair. Moreover, osteochondral defect models are invaluable for assessing integration of a tissue engineered graft with the surrounding cartilage, which is critical for its function and presents a significant challenge in the field. Several materials have been proposed to improve cartilage integration; nevertheless, inadequate biomechanical stability of the graft has often been observed, demonstrating the need for improved treatments [24,26].

Another parameter that needs more rigorous pre-clinical testing is the pre-culture time of an engineered cartilaginous construct, as this was shown to play a pivotal role for both maturation and tissue integration upon implantation [27]. The ideal stage of development is still unknown, and it is most likely scaffold dependent. Despite there are disparate factors that obstacle cartilage integration [28], the mechanical loading is a function conditioner to enhance lateral integration following cartilage repair, which is likely to be the determining factor in the clinical success of the repaired tissue [29]. However, common osteochondral *ex vivo* models have not taken into account the mechanical component and therefore lack an important physiological stimulus; while standard bioreactor studies have applied load to isolated hydrogels or scaffolds mostly in unconfined mode and have not considered the confined environment within the tissue that is experienced *in vivo*. The present study for the first time combines an osteochondral defect model with mechanical compression and shear load that simulates physiological joint kinematics. Addition of multi-axial mechanical load to this model represents an important advancement, enabling more predictive pre-clinical screening of novel therapies and biomaterial-based implants, thereby replacing or reducing pre-clinical *in vivo* animal studies.

Furthermore, using functioning human cells or tissues to screen treatment candidates could accelerate the development process and provide key tools for more clinically relevant research. Organ culture bioreactors therefore hold the potential to provide a testing platform that is more predictable of the whole tissue response, facilitating the therapy screening before starting the clinical trial [30].

The aims of this study were 1) to evaluate the osteochondral explant vitality and cartilage integrity under combined compression and shear load and (2) to assess the early cellular responses to multi-axial load in a confined microenvironment, using an established fibrin-polyurethane scaffold. We demonstrate that cartilage and bone remain viable over the 10 days culture period. Furthermore, we confirm the applicability of the osteochondral defect model with a cell-scaffold construct under mechanical stimuli in a joint bioreactor system.

## 2. Material and methods

### 2.1. Osteochondral tissue harvest, defect creation and culture

Osteochondral explants were harvested from stifle joints of 3 to 5-months-old calves, obtained from a local abattoir (Metzgerei Angst AG, Zurich, CH) within 48 h of slaughter. Joints were dissected to expose the patellar groove and examined for absence of cartilage bruising and blood tint. Cylindrical osteochondral explants were obtained with an 8 mm diameter diamond coated custom-made trephine drill (Peertools AG, Ftan, CH), using a Bosch compact drill press, saline irrigation and a manual circular saw (Fig. 1A). The machine was equipped with an adjustable table for round and angular stifle joint positioning and achieved vertical cutting. Variable speed control and digital drilling depth monitoring facilitated obtainment of a flat articular cartilage surface in a reproducible manner. The subchondral bone part was trimmed to obtain a final osteochondral explant height of 6 mm. From each stifle joint, 5 osteochondral explants were obtained (Fig. 1B).

To generate osteochondral defects, a 4 mm trephine drill was used (Brusch-Ruegger, Urdorf, CH, Fig. 1C) to centrally remove a full thickness circular cartilage biopsy including part of the subchondral bone (Fig. 1D). To determine the consistency of the harvesting, diameter and length of osteochondral explants were measured using a calliper (Mitutoyo Absolute Digimatic Caliper range 0/200 mm). Subsequently, explants were cultured in Dulbecco's modified eagle medium (DMEM-HG, 4.5 g/L-glucose; Gibco) supplemented with 10% fetal bovine serum (FBS, Gibco) and penicillin/streptomycin (1% P/S, Gibco), at 37 °C and 5% CO<sub>2</sub>. Intact osteochondral explants and osteochondral defect models were incubated overnight to ensure sterility. Then they were placed in custom-made bioreactor sample holders containing 2% low-gelling agarose (SeaPlaque Agarose, Lonza, Rockland, USA), to cover the bone part and prevent cell outgrowth from the subchondral bone, and cultured in DMEM-HG, 1% insulin-transferrin-selenium (ITS), non-essential amino acids and 1% P/S. The medium, referred to as chondro-permissive medium, was changed three times per week.

### 2.2. Chondrocytes-polyurethane scaffold constructs

Cylindrical (4.15 mm x 2.3 mm and 4.15 mm x 4.3 mm) polyurethane (PU) scaffolds (average pore size 150–300  $\mu$ m) were prepared as described previously [31–33]. Scaffolds were sterilized by ethylene oxide exposure for 4 h at 37 °C and subsequently degassed at 45 °C and 150 mbar for 4 days. Before cell seeding, scaffolds were pre-incubated in DMEM-HG supplemented with 1% P/S for 1 h to wet the hydrophobic polymer. Chondrocytes were

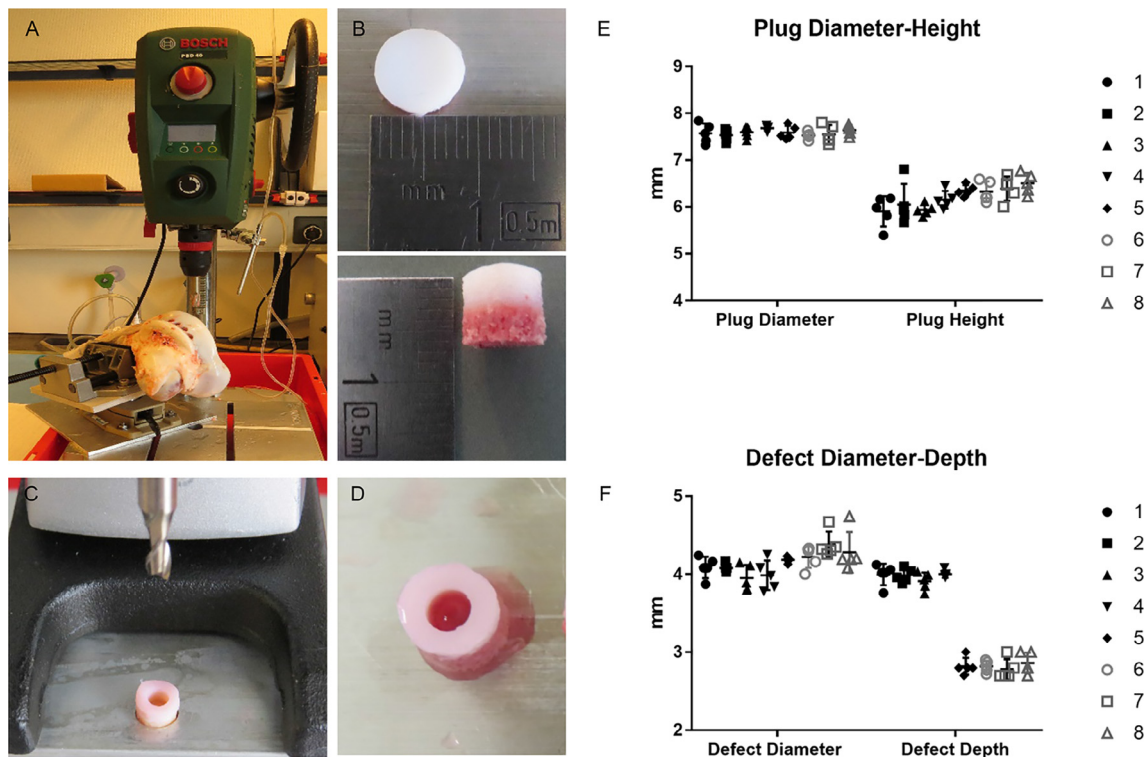


**Fig. 1.** Reproducibility of osteochondral harvesting and defect creation. (A) Compact drill press, which achieves vertical cutting, and an angle adjustable table for bovine stifle joint positioning. (B) Representative image of an osteochondral explant harvested from the femoral groove; the bone was trimmed to reach the desired height. (C) The trephine (4 mm diameter) is adjusted for creating the desired depth of the circular groove, controlled by the digital drilling press. (D) Representative image of osteochondral defect model. (E) Results of intact osteochondral explant diameter and height achieved after drilling and trimming (F) Results of osteochondral defect diameter and depth, showing two different cartilage height groups. Data are presented as mean  $\pm$  SD (from 8 stifle joints, n = 5 per joint).

isolated from the left femoral condyles [34], using pronase and sequential collagenase digestion as previously described [35]. Upon isolation, primary bovine chondrocytes were suspended in fibrinogen solution and then mixed with thrombin solution (both from Baxter, Vienna) immediately prior to seeding into the PU scaffold at a cell density of  $5 \times 10^7$ /mL. The final concentrations of the fibrin gel components were 17 mg/mL fibrinogen and 0.5 U/mL thrombin [36]. Constructs were incubated for 1 h at 37 °C, 5% CO<sub>2</sub> to permit fibrin gelation before adding them into the osteochondral defect and were then cultured in chondro-permissive medium, containing 500 kIU/mL aprotinin to prevent fibrin degradation (Fluka, Buchs, Switzerland). The addition of 50  $\mu$ g/mL ascorbic acid was delayed until 5 days post-seeding, in order to avoid cell damage due to oxidative stress directly after enzymatic digestion during chondrocytes isolation [37].

### 2.3. Mechanical loading

After 5 days of pre-culture, osteochondral defect models filled with cell-scaffold constructs underwent mechanical stimulation using our four-station bioreactor system, installed in a CO<sub>2</sub> incubator at 37 °C, 5% CO<sub>2</sub>, 85% humidity [38]. A commercially available ceramic hip ball (32 mm in diameter) was pressed onto the osteochondral explants to provide a constant displacement of 0.4 mm or 10% to 14% of the cartilage height (in the centre), to fully maintain the contact of the ball with the cell-scaffold constructs and the surrounding cartilage. Loading groups were exposed to axial compression in a sinusoidal manner between 0.4 mm and 0.8 mm, resulting in an actual strain amplitude of 10–20% or 14–26% of the cartilage explant height (depending on the cartilage height group; see 3.1) at a frequency of 0.5 Hz and simultaneous shear motion by ball oscillation at  $\pm 25^\circ$  and 0.5 Hz. The maximal mechanical loads

applied corresponded to 15 N or approximately 0.35 MPa (Fig. 2A, B). This regime of dynamic axial compression with superimposed sliding motion is suggested to more closely simulate joint articulation compared to axial compression [39].

One hour of mechanical loading was performed twice per day (8 h free-swelling between loading cycles) over 5 consecutive days. In between loading cycles, samples were kept in free-swelling condition (without ball contact) and medium was collected at the end of the experiment to assess the glycosaminoglycan (GAG) release. Free-swelling osteochondral defect models with cell-scaffold constructs served as controls.

### 2.4. Validation of the model: Viability assay

Cell viability of the osteochondral explants was monitored at day 0 (directly after harvesting) and at day 10 by lactate dehydrogenase (LDH) – ethidium homodimer staining. For thin sections, samples were snap-frozen and stored at  $-80^\circ\text{C}$ . A tungsten carbide D-blade (MICROM, 16 cm, cat. num. 152120) was used to obtain sagittal cryo-sections (20  $\mu$ m) of undecalcified osteochondral defect models and intact osteochondral explants. Briefly, slides were rinsed in phosphate buffered saline (PBS) and incubated with ethidium-homodimer (46043 SMG-F, Sigma) in PBS for 30 min at 37 °C. Subsequently, sections were rinsed in PBS and stained with 40% Polypep-based LDH solution using the salt nitroblue tetrazolium (NBT) as third substrate next to lactate and nicotinamide adenine dinucleotide (NAD) for 3 h at 37 °C. To assess bone viability, thick sections (250  $\mu$ m) were cut with an annular saw (Leica) and stained with 5% Polypep-based LDH solution using the above-mentioned substrates [40]. Sections were mounted with water based mountant and imaged using a fluorescence microscope to assess the presence of dark stained chondrocytes and osteocytes.



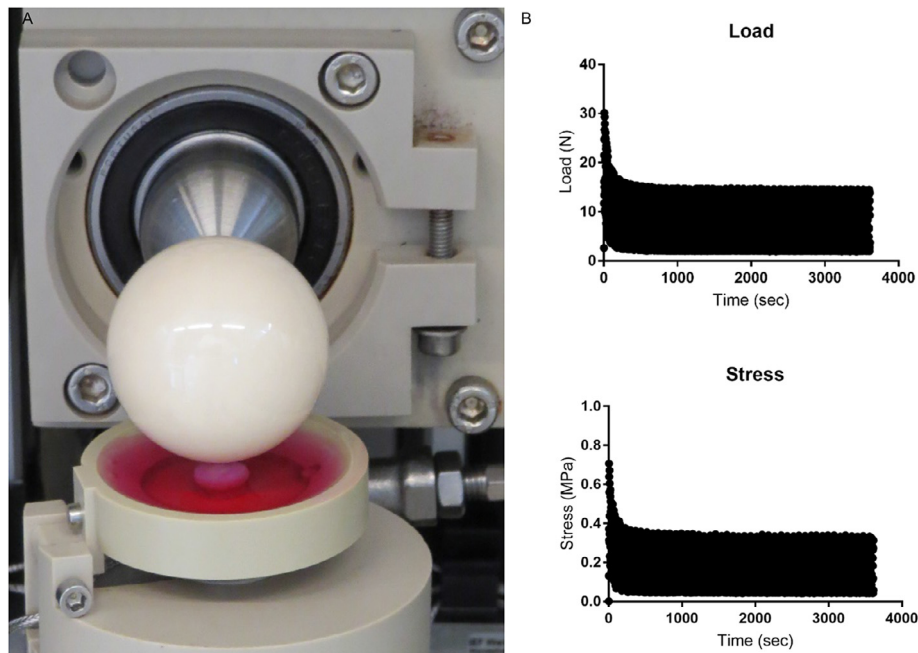


**Fig. 2.** Loading applied to osteochondral defect model. (A) Representative image of one station of the joint bioreactor that allows for application of joint specific biomechanical stimuli to osteochondral defect models. Cartilage defect was filled with chondrocytes-seeded scaffold. (B) Maximal mechanical load applied to the osteochondral explant measured in newton (N) and respective stress in megapascal (MPa). Representative graphs of one osteochondral defect model at day 10 of culture (5 days of mechanical loading), after one hour of loading.

## 2.5. Histology

Histological samples were fixed in 4% buffered formaldehyde (Formafix AG, Hittnau, CH) for 48 h, decalcified in 10% formic acid (Fluka, cat.num.06460) for 6 days, then embedded in paraffin and sectioned in 5  $\mu$ m sections. For staining, slides were deparaffinised using xylene and subsequently hydrated. Safranin O/Fast green staining was performed to visualize proteoglycan and collagen content. Briefly, slides were first stained with Weigert's Haematoxylin for 10 min, blued in tap water for 10 min, stained with 0.002% Fast green in deionized water for 5 min and washed in 1% acetic acid. Then, sections were stained with 0.1% Safranin O for 12 min.

## 2.6. RNA extraction and gene expression analysis

At the end of the experiment, cell-scaffold constructs were removed from the osteochondral defect model, homogenized using the Tissue Lyser system (Qiagen, Retsch, Germany), and total RNA was extracted using TRI Reagent® (Molecular Research Center, Cincinnati, OH). Reverse transcription was performed with TaqMan® reverse transcription reagents (Thermo Fisher Scientific,

Reinach, Switzerland), using random hexamer primers and 1  $\mu$ g of total RNA. Table 1 shows the sequences of bovine primers and TaqMan probes for collagens type-I (*COL1A2*), type-II (*COL2A1*), aggrecan (*ACAN*), cartilage oligomeric matrix protein (*COMP*), proteoglycan 4 (*PRG4*/Lubricin), matrix metalloproteinase 3 (*MMP-3*) and *MMP-13*. Primers and probe for amplification of ribosomal protein lateral stalk subunit P0 (*RPLP0*, Bt03218086\_m1) and Versican (*VCAN*, Bt03217632\_m1) were from Applied Biosystems (Rotkreuz, Switzerland). Relative quantification of target mRNA was performed according to the comparative  $C_T$  method with bovine *RPLP0* as the endogenous control. For a given amount of total RNA, *RPLP0* values did not vary among the different groups, confirming *RPLP0* was an appropriate endogenous control for chondrocytes-PU constructs subjected to mechanical stimuli. Data were further normalized to the values of the unloaded controls and converted to relative mRNA values using the  $2^{-\Delta\Delta C_T}$  method [41].

## 2.7. Biochemical analysis: s-GAG and DNA content

Cell-scaffold constructs (removed from osteochondral defect models) and media were collected for biochemical analysis. Chondrocytes-scaffold constructs were digested overnight in

**Table 1**  
Oligonucleotide primers and probes used for qRT-PCR.

Gene	Primer forward (5'-3')	Primer reverse (5'-3')	Probe (5'-FAM-3'-TAMRA)
Collagen 1A2	TGC AGT AAC TTC GTG CCT AGC A	CGC GTG GTC CTC TAT CTC CA	CAT GCC AAT CCT TAC AAG AGG CAA CTG C
Collagen 2A1	AAG AAA CAC ATC TGG TTT GGA GAA A	TGG GAG CCA GGT TGT CAT C	CAA CGG TGG CTT CCA CTT CAG CTA TGG
Aggrecan	CCA ACG AAA CCT ATG ACG TGT ACT	GCA CTC GTT GGC TGC CTC	ATG TTG CAT AGA AGA CCT CGC CCT CCA T
MMP-3	GGC TGC AAG GGA CAA GGA A	CAA ACT GTT TCG TAT CCT TTG CAA	CAC CAT GGA GCT TGT TCA GCA ATA TCT AGA AAA C
MMP-13	CCA TCT ACA CCT ACA CTG GCA AAA G	GTC TGG CGT TTT GGG ATG TT	TCT CTC TAT GGT CCA GGA GAT GAA GAC CCC
COMP	CCA GAA GAA CGA CGA CCA GAA	TCT GAT CTG AGT TGG GCA CCT T	ACG GCG ACC GGA TCC GCA A
PRG4	GAG CAG ACC TGA ATC CGT GTA TT	GGT GGG TTC CTG TTT GTA AGT GTA	CTG AAC GCT GCC ACC TCT CTT GAA A

0.5 mg/mL proteinase K at 56 °C (2.5 U/mg, chromozyme assay; Roche, Mannheim, Germany). DNA content was measured using QUANT-iT<sup>®</sup> Picogreen, ds assay kit (Molecular Probes, Life Technologies), and values were normalized per scaffold volume. The total amounts of sulfated glycosaminoglycan (s-GAG) retained within the scaffold constructs and released from the osteochondral defect models into the media were determined by the dimethyl-methylene blue (DMMB) dye-binding assay [42].

### 2.8. Statistical analysis

The results are expressed as mean  $\pm$  standard deviation (SD) of 3 experiments with different chondrocyte donors. s-GAG, DNA content and qPCR data were statistically analysed using non-parametric testing (Mann Whitney *U* test), since the data were not normally distributed. Differences were considered statistically significant for  $p < 0.05$ .

## 3. Results

### 3.1. Validation of the osteochondral model generation

To validate the generation of the osteochondral defect model, measurements were taken to evaluate the osteochondral explant obtainment and the reproducibility of the defect creation. It is worth noting that having this procedure standardized is of critical importance for the mechanical loading set up. Explants obtained from stifle joints harvested from 8 calves had an average diameter of 7.60 mm and height of 6.10 mm, with standard deviations of

0.14 mm and 0.29 mm, respectively (Fig. 1E). Cartilage height was measured to define the depth of osteochondral defects; the height varied between approximately 3 mm and 4 mm, depending on the bovine donor. Cylindrical holes were created with depths of 2.85 mm  $\pm$  0.11 mm for the 3 mm cartilage height group, or 3.75 mm  $\pm$  0.30 mm for the 4 mm cartilage height group and were 4.30 mm  $\pm$  0.16 mm in diameter (Fig. 1F). Depths were measured from the upper rim of the cartilage by a custom-made crown mill to the level of the circular groove made. In all cases measured, a reproducible procedure was observed. Coefficients of variation of the intact osteochondral explant diameter and height ( $n = 40$ ), and defect diameter and depth are shown in Table 2.

### 3.2. Evaluation of osteochondral cells morphology and viability after mechanical stimulation

To verify the viability of the cells in the osteochondral defect models, with or without exposure to mechanical stimuli, LDH/ethidium homodimer positive cells were determined after samples collection at day 0 and after 10 days of culture. Cells within both cartilage and bone regions remained viable throughout the culture period (Fig. 3A, B), except for a small zone of cell death in the outermost cell layer at the cut edges of the cartilage and the edges of the defect for all samples (Fig. 3A). The loading regime did not affect cell viability in comparison to the free-swelling controls. Safranin O Fast Green staining revealed normal proteoglycan distribution (Fig. 4A), GAG measurement in the medium indicated that the mechanical stimuli did not wear out the cartilage GAG, as no difference in GAG release into the media was detected in comparison to the free swelling controls (Fig. 4B). Chondrocytes maintained their typical morphology, with rounded and polygonal shape in both conditions (Fig. 4A).

### 3.3. Physical stimulation of chondrocytes-seeded scaffold in osteochondral defect models

To test the biological response of chondrocytes-seeded scaffolds implanted into the osteochondral defect model to mechanical loading, DNA, GAG content and mRNA expression levels of the constructs were quantified after 5 days of loading (Figs. 5, 6).

**Table 2**  
Coefficients of variation of intact osteochondral explants and osteochondral defect models.

Osteochondral Explant	Coefficient of Variation (%)
Height	4.99
Diameter	1.76
Osteochondral Defect Model Diameter	4.78
Osteochondral Defect Model Depth (High)	2.47
Osteochondral Defect Model Depth (Low)	3.76

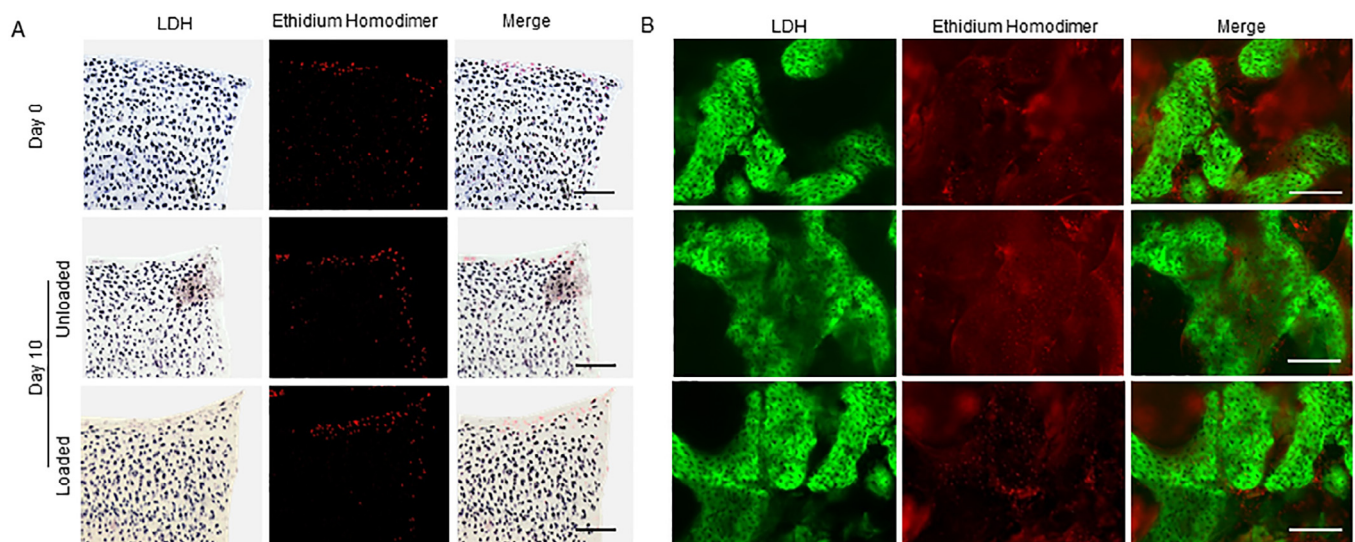


**Fig. 3.** Osteochondral explant viability. Representative images of LDH/Ethidium homodimer stained cells at day 0 and day 10 for unloaded and loaded samples, (A) in the cartilage (B) in the bone. Scale bars indicate 200  $\mu$ m (dark-blue cells and double-stained cells = LDH positive cells, representing living cells; red cells = Ethidium Homodimer positive cells, representing dead cells; green is bone autofluorescence, 515–565 nm emission filter [40]). (For interpretation of the references to colour in this figure legend, the reader is referred to the web version of this article.)

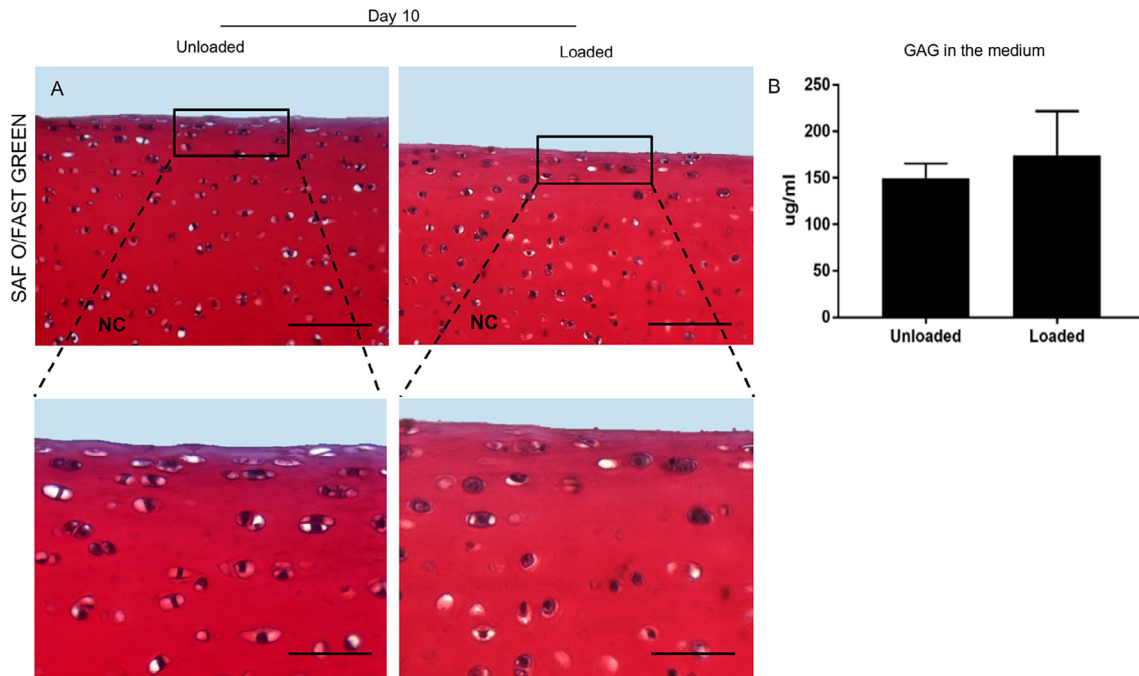


**Fig. 4.** Effect of loading on articular cartilage. (A) SAF-O/Fast Green stained osteochondral biopsies. Detail images of articular cartilage after 10 days of culture for unloaded and loaded samples, respectively; 20× magnification, scale bars indicate 100 μm. Dashed lines indicate sections at 40× magnification, scale bars are 50 μm. (B) GAG release into the medium at day 10 of culture. Data are presented as mean  $\pm$  SD (3 donors, n = 12 per group). NC: Native cartilage. (For interpretation of the references to colour in this figure legend, the reader is referred to the web version of this article.)

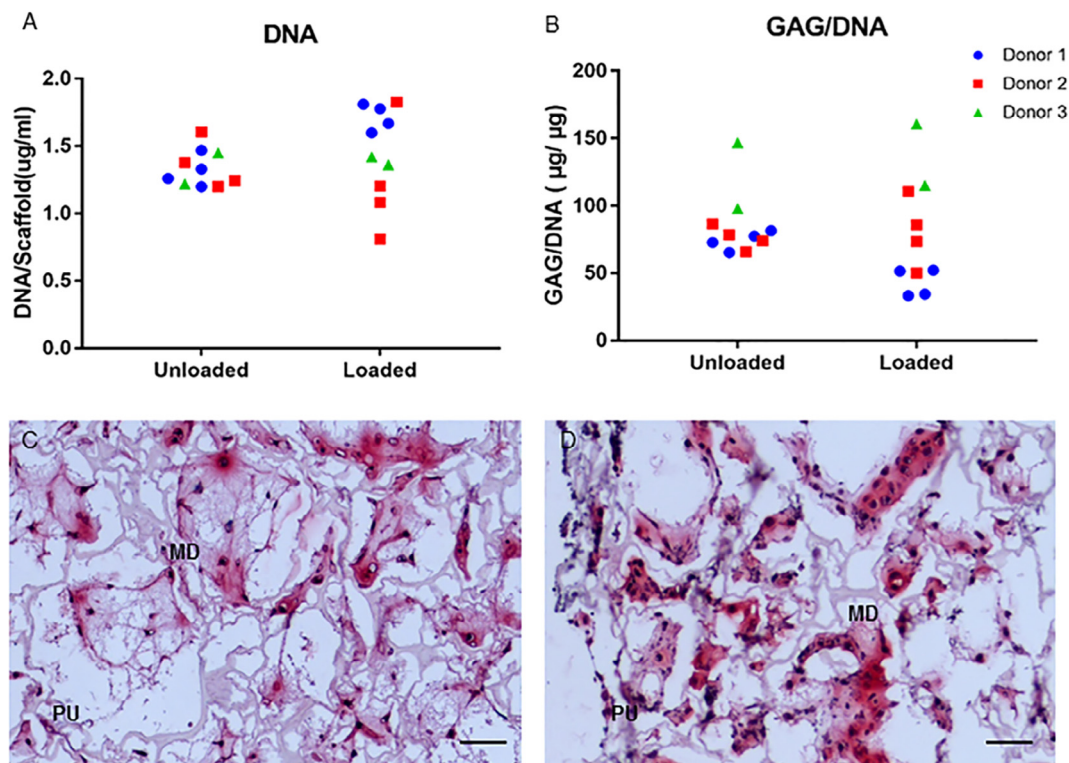


**Fig. 5.** DNA and GAG content in chondrocyte seeded scaffolds in osteochondral defect models cultured in the bioreactor. (A) DNA content of unloaded and loaded chondrocytes seeded polyurethane scaffolds cultured for 10 days. (B) GAG per DNA ratio of unloaded and loaded chondrocytes seeded polyurethane scaffolds cultured for 10 days. (C, D) detail images of PU scaffolds stained with Safranin O/Fast Green after 10 days of culture for unloaded (C) and loaded samples (D), respectively; scale bars indicate 50 μm. Results from 3 chondrocyte donors assessed in duplicates (donor 3) or quadruplicates (donors 1 and 2) are shown. PU: Polyurethane scaffold, MD: Matrix deposition. (For interpretation of the references to colour in this figure legend, the reader is referred to the web version of this article.)



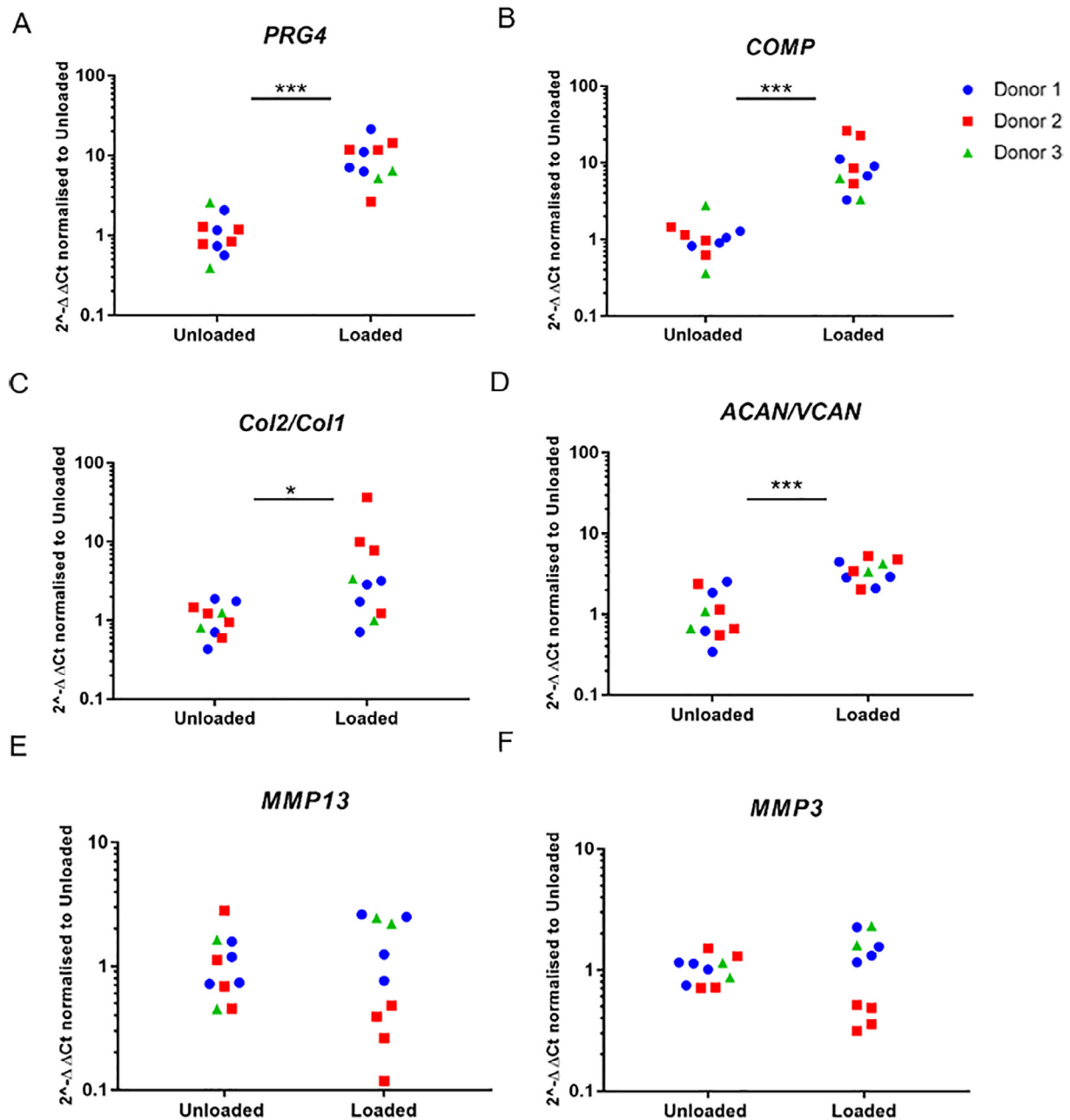


**Fig. 6.** Effect of articular motion on the chondrocytic phenotype. (A–F) mRNA expression of chondrocytes seeded into polyurethane scaffolds, implanted in the osteochondral defect, and exposed to dynamic compression and surface motion. Data are expressed relative to mRNA levels of unloaded constructs. Results from 3 chondrocyte donors assessed in duplicates (donor 3) or quadruplicates (donors 1 and 2) are shown; \* $p < 0.05$ , \*\*\* $p < 0.001$ .

Cell-scaffold constructs which underwent loading contained similar amounts of DNA as the unloaded controls (Fig. 5A). GAG content normalised to DNA was stable between the groups, indicating no effect of the loading on GAG production per cell (Fig. 5B). This was confirmed by Safranin O/Fast Green staining of scaffold constructs, where similar amounts of matrix deposition were observed in both groups (Fig. 5C, D).

The mRNA expression levels of *PRG4*/Lubricin and *COMP* were significantly enhanced in cell-scaffold constructs exposed to complex load as compared to unloaded controls (8.4 and 9-fold increase, respectively;  $p < 0.001$ , Fig. 6A, B). The mRNA ratios of *COL2A1* to *COL1A2* and of *ACAN* to *VCAN*, defined as indices of chondrocytes differentiation, were significantly higher in loaded samples compared to free-swelling controls ( $p = 0.015$  and  $p < 0.001$ ,

respectively) (Fig. 6C, D). The gene expression levels of metalloproteinases *MMP3* and *MMP13* remained relatively stable; considering donor variations no significant differences were observed between the groups (Fig. 6E, F).

#### 4. Discussion

Considering articular cartilage as load bearing tissue, multi-axial stimuli applied to an *ex vivo* osteochondral defect model are important parameters to investigate their effects on the cartilage repair process. The present study showed that osteochondral defect models, in which mechanical loads were applied: 1) were viable after 5 days of pre-culture and 5 days within the complex

motion bioreactor culture based on LDH staining, 2) did not exhibit articular surface wear as assessed by Safranin O/Fast Green staining and GAG release into the media; and 3) maintained typical gene expression responses (*PRG4*/Lubricin and *COMP*) to load in primary chondrocytes seeded into polyurethane scaffolds filling the osteochondral defects. Further, we showed that reproducible defects could be created at the desired depth. This was reflected by the coefficients of variation that were <4% for both depth and diameter. Earlier described osteochondral defect models did not precisely document the control of the defect depth [25,43,44]; others directly implanted the osteochondral biopsies *in vivo* [45,46]; but to our knowledge none of them were intended for *ex vivo* mechanobiology and regenerative studies under complex articulating motion [47–49].

No detrimental effect of mechanical load on the cartilage samples was observed. Both histology and GAG release into the medium of the loaded group did not show significant differences compared to the free swelling control group. This finding indicates more favorable outcomes in terms of matrix wear and tissue preservation compared to other *ex vivo* studies with complex motion [50] or animal models [51,52], which used metal articulating indenters or implants to mimic the situation after surgery (e.g. hemiarthroplasty). Surface chemistry and roughness of metal implants can increase friction against articular cartilage and can have significant influence on tissue integrity [53]. Overall, chondrocytes viability was mostly preserved by using saline irrigation for cooling when generating the explants, and no difference in cell death was found in osteochondral explants that underwent compression and shear stress compared to controls; nevertheless, minimal chondrocytes death was observed at the outermost edges of the osteochondral explant and of the defect, as previous works already described [54,55]. This observation might be representative of a clinical cartilage defect where dead cells have been found along the edges of the injury following joint trauma [56]. Furthermore, a zone of chondrocyte death has been described in and around the periphery of osteochondral grafts that could be reduced by the application of growth factor and collagenase [57]. Therefore, this model could also be very interesting to study such clinically relevant aspects.

Although our model still does not match the native whole joint situation, the application of complex motion patterns using a ceramic ball and the implementation of osteochondral defects bring it one step closer to a more physiologically relevant system compared to cartilage explants alone [39]. Dynamic compression and ball oscillation drag flow into the osteochondral defects filled with chondrocytes-PU constructs, resulting in the activation of mechano-transduction pathways, which severely depend on the type of load [58]. The loading protocol was chosen based on a protocol previously described by our group: Grad et al. investigated the effect of unidirectional and multidirectional motion patterns on gene expression and molecule release of bovine chondrocytes-seeded polyurethane scaffolds [20]. After 5 days of loading, as in the present work, results showed that multidirectional loading consisting of axial compression and ball oscillation, promoted the maintenance of the chondrocytic phenotype through upregulation of chondrogenic gene expression.

The oscillation frequency was set at 0.5 Hz, which is higher than the 0.1 Hz used in the previous study. Our previous evaluation of the effect of sliding velocity on the response of chondrocytes in 3D scaffolds revealed that higher frequency generally triggered a more pronounced response [59]. Accordingly, 1 Hz frequency which approximates the frequency of compressive loading the human articular cartilage experiences during walking and running conditions, induced greatest gene expression upregulation. Interestingly, increasing the frequency from 0.1 to 1 Hz also improved the induction of chondrogenesis in mesenchymal stem cell seeded

scaffolds exposed to multiaxial loading [21]. Here, we slightly reduced the loading frequency to 0.5 Hz to minimize the articular cartilage surface injury [60] in the osteochondral model.

The results of this study demonstrated a marked increase in *PRG4* gene expression in the loaded group (9-fold higher compared to unloaded), which is in line with previous studies on the effects of complex load on articular chondrocytes [19,20]. The higher response of *PRG4* compared to previous results may be related to: a different oscillation frequency of the ceramic ball, different impact of the sliding velocity at the new articular cartilage-PU interface [59] and the more confined system, in which the chondrocytes could sense different stress distribution within the scaffold [61]. In the fibrin-polyurethane composite scaffolds, hydrostatic pressure buildup due to the application of external loading would be negligible in an unconfined system because of the high permeability of the scaffolds [61]. In the current confined system, certain hydrostatic pressure is built up, which has been shown to promote chondrogenesis, though the effect of pure hydrostatic pressure on *PRG4* expression of chondrocytes has not been investigated [62]. Consistent with previous findings [20], the influence of oscillating surface motion also promoted the upregulation of *COMP* (8.4-fold increase), one of the most abundant non-collagenous proteins of the cartilage ECM. Earlier studies exploring the influence of uni- and multi-axial loading on gene expression in chondrocytes-seeded polyurethane scaffolds demonstrated that the induction of *COMP* gene expression depended on the loading type and velocity. Axial compression alone did not affect *COMP* mRNA expression, whereas compression and superimposed sliding motion by ball oscillation significantly increased *COMP* mRNA levels [20]. Besides, increasing sliding velocity triggered more pronounced up-regulation of *COMP* gene expression [59]. Furthermore, an increase in the mRNA ratios of Collagen II to Collagen I and Aggrecan to Versican, defined as markers of chondrocytes differentiation [63], was also associated with the application of compression and shear. These data suggest that physiological stimuli are essential for stimulation of the chondrogenic phenotype and, more indirectly, for cartilage matrix formation and organization, despite the total GAG per DNA did not show variations between the two groups. Longer term repetitive loading may be necessary to induce significant effects on matrix production [18]. The joint motion simulator did not affect the gene expression of the two matrix degrading enzymes, *MMP3* and *MMP13*, that are involved in joint pathologies. This indicates that mechanical stimuli did not specifically foster collagenase-induced extracellular matrix degradation in chondrocytes implanted into osteochondral biopsies.

A chondrocytes-seeded hybrid fibrin-polyurethane scaffold was used as a model implant in this study. The fibrin component served to improve the cell and matrix retention and to better promote the chondrocytic phenotype compared to the macro-porous PU structure alone [36]; while the elastic PU scaffold has been shown to favorably transmit the applied dynamic mechanical loads [58]. Nevertheless, this material faces some limitations, such as the slow rate of ECM accumulation in the construct center. Other promising materials, for instance injectable thermo-reversible methylcellulose-based hydrogels [64], modified hyaluronic acid hydrogels functionalized with biochemical gradients [65] or biopolymers with improved tissue adhesion properties [66] will be envisaged in future studies.

The model has the advantage of having the cartilage-bone unit intact. Cartilage and bone have been demonstrated to influence each other, and it is known that not only the cartilage but also bone responds to mechanical stimulation to preserve the mechanical strength and impede demineralization [67]; thus, this loaded osteochondral model provides the possibility to recapitulate the healing process in a joint-like microenvironment. There is a body



of evidence suggesting that these tissues can communicate. For example, the interface between the subchondral bone and calcified cartilage contains numerous vascular canals suggesting a potential route for molecular diffusion between the two compartments [68–70]. The model can also be used to study the effect of bone changes (that occur in joint diseases such as marrow lesions or subchondral sclerosis) on cartilage repair. Further optimization might include the addition of hyaluronic acid in the bioreactor culture to better mimic the joint space [71]. Another adaptation to the model that can be envisaged is the development of a cartilage-on-cartilage articulating motion system [39], which will better resemble the natural joint niche and will reduce the friction of the testing system. While the present study allowed us to assess the early cellular response to multiaxial load in a confined system, longer studies over at least 3 weeks would be required to achieve neo-cartilage formation by accumulation of significant amounts of extracellular matrix within the cell-seed implants. The short observation time does not allow us to draw conclusions about the implant integration into the host tissue. Nevertheless, we showed the medium-term survival and integrity of the cartilage-bone explant and the reaction of the implanted cells to the applied load, which warrants future long-term studies with advanced cell-material constructs.

Several applications are possible: cartilage repair treatments could be screened *ex vivo*, for example to test the potential of different cell sources and new biomaterials denoting their capabilities to promote chondrogenesis and to integrate into the native tissue. In addition, recruitment of endogenous cells from cartilage or underlying bone into the osteochondral defect and migration of these cells into a biomaterial can be studied with or without the addition of chemokines or growth factors to stimulate tissue repair as cell-free cartilage repair strategy [72]. The system can also perform continuous passive motion with intermittent active motion and hence improve our understanding on the post-operative management of joint injuries and on the time of convalescence, since post-operative loading also affects the quality of the cartilage surgery outcome [73].

We also believe that the *ex vivo* bioreactor-osteochondral culture model may represent an alternative pre-clinical testing system to evaluate the potential and limitations of different treatment approaches prior moving to *in vivo* testing, in order to minimize the number of animals needed. Where animal testing cannot be replaced, *ex vivo* bioreactor cultures could contribute to identify the proper animal species, the suitable number of animals and to find biologically and statistically relevant differences among groups [30]. A multi-center analysis has shown low correlation between *in vitro* cell culture and *in vivo* biomaterial testing for bone regeneration [74]; hence, pilot studies could be performed *ex vivo* with explants from animals of the same species to help bridging this gap. Furthermore, with this model human tissue can be tested, which is an unprecedented opportunity to be clinically relevant.

Nonetheless, the osteochondral defect model under load faces certain limitations. As it does not resemble the entire diarthrosis, it is not possible to replicate the whole range of events determining the body's healing response in cartilage repair *in vivo*. The wound healing process is significantly affected by the synovium and synovial fluid, which play a significant role in nutrient supply, metabolic by-product clearance and immune response, thereby influencing matrix production [75]. A critical element in cartilage healing is also the defect size. A rabbit model has shown that different diameters of osteochondral defects heal differently [76]. Our present system only partially reproduces human osteochondral lesions, which can be at least 2 cm<sup>2</sup>; therefore, the smaller defect repair may not exactly indicate the cell behaviour adopted in a larger defect. Minor modification of our current model will be required to address also large defect sizes. Last, our bioreactor

does not perfectly mimic the complex joint kinematics; rolling or moving contact has not been implemented in our system, which is another important motion component.

In conclusion, we have established a novel *ex vivo* osteochondral defect culture model in a mechanically stimulated microenvironment. Such a model has both experimental and clinical relevance; it can serve to further elucidate the biological and physical crosstalk among the subchondral bone and cartilage in the recovery of osteochondral defects and may help to reveal the molecular signaling involved in the repair in response to a treatment. It will also prove its efficiency regarding controlling cartilage repair under the influence of different loading protocols. Longer-term studies over several weeks will be performed to monitor and evaluate cell and biomaterial-guided neo-cartilage formation and neo-tissue integration using novel cartilage repair methods.

## Acknowledgment

We thank David Eglin for producing the polyurethane scaffolds.

## Funding source

This project has received funding from the European Union's Horizon 2020 research and innovation programme under Marie Skłodowska-Curie Grant Agreement No 642414.

## Disclosures

All authors declare they have no conflict of interest.

## References

- [1] S.W. O'Driscoll, F.W. Keeley, R.B. Salter, Durability of regenerated articular cartilage produced by free autogenous periosteal grafts in major full-thickness defects in joint surfaces under the influence of continuous passive motion. A follow-up report at one year, *J. Bone Joint Surgery Am.* 70 (4) (1988) 595–606.
- [2] L.L. Johnson, Arthroscopic abrasion arthroplasty historical and pathologic perspective: present status, *Arthroscopy J. Arthroscopic Related Surgery Official Publ. Arthroscopy Assoc. N. Am. Int. Arthroscopy Assoc* 2 (1) (1986) 54–69.
- [3] M. Brittberg, Autologous chondrocyte transplantation, *Clin. Orthopaedics Related Res.* 367 Suppl (1999) S147–S155.
- [4] M. Brittberg, A. Lindahl, A. Nilsson, C. Ohlsson, O. Isaksson, L. Peterson, Treatment of deep cartilage defects in the knee with autologous chondrocyte transplantation, *New England J. Med.* 331 (14) (1994) 889–895.
- [5] S.D. Gillgoly, M. Voight, T. Blackburn, Treatment of articular cartilage defects of the knee with autologous chondrocyte implantation, *J. Orthopaedic Sports Phys. Ther.* 28 (4) (1998) 241–251.
- [6] R.J. Williams 3rd, H.W. Harnly, Microfracture: indications, technique, and results, *Instr. Course Lect.* 56 (2007) 419–428.
- [7] R. Dorotka, U. Windberger, K. Macfelda, U. Bindreiter, C. Toma, S. Nehrer, Repair of articular cartilage defects treated by microfracture and a three-dimensional collagen matrix, *Biomaterials* 26 (17) (2005) 3617–3629.
- [8] J.R. Steadman, W.G. Rodkey, J.J. Rodrigo, Microfracture: surgical technique and rehabilitation to treat chondral defects, *Clin. Orthopaedics Related Res.* 391 Suppl (2001) S362–S369.
- [9] R.J. Bergman, D. Gazit, A.J. Kahn, H. Gruber, S. McDougall, T.J. Hahn, Age-related changes in osteogenic stem cells in mice, *J. Bone Mineral Res. Official J. Am. Soc. Bone Mineral Res.* 11 (5) (1996) 568–577.
- [10] A. Stolzinger, A. Scutt, Age-related impairment of mesenchymal progenitor cell function, *Aging Cell* 5 (3) (2006) 213–224.
- [11] A. Chetty, T. Steynberg, S. Moolman, R. Nilen, A. Joubert, W. Richter, Hydroxyapatite-coated polyurethane for auricular cartilage replacement: an *in vitro* study, *J. Biomed. Mater. Res. Part A* 84 (2) (2008) 475–482.
- [12] B.H. Ruszymah, B.S. Lokman, A. Asma, S. Munirah, K. Chua, A.L. Mazlyzam, M.R. Isa, N.H. Fuzina, B.S. Aminuddin, Pediatric auricular chondrocytes gene expression analysis in monolayer culture and engineered elastic cartilage, *Int. J. Pediatr. Otorhinolaryngol.* 71 (8) (2007) 1225–1234.
- [13] J.S. Temenoff, A.G. Mikos, Review: tissue engineering for regeneration of articular cartilage, *Biomaterials* 21 (5) (2000) 431–440.
- [14] H. Chiang, C.C. Jiang, Repair of articular cartilage defects: review and perspectives, *J. Formosan Med. Assoc.* =Taiwan yi zhi 108 (2) (2009) 87–101.
- [15] K. Bobacz, L. Erlacher, J. Smolen, A. Soleiman, W.B. Graninger, Chondrocyte number and proteoglycan synthesis in the aging and osteoarthritic human articular cartilage, *Ann. Rheum. Dis.* 63 (12) (2004) 1618–1622.

- [16] A.R. Tan, C.T. Hung, Concise Review: Mesenchymal Stem Cells for Functional Cartilage Tissue Engineering: Taking Cues from Chondrocyte-Based Constructs, *Stem Cells Transl. Med.* 6 (4) (2017) 1295–1303.
- [17] S. Grad, D. Eglin, M. Alini, M.J. Stoddart, Physical stimulation of chondrogenic cells in vitro: a review, *Clin. Orthop. Relat. Res.* 469 (10) (2011) 2764–2772.
- [18] E. Wernike, Z. Li, M. Alini, S. Grad, Effect of reduced oxygen tension and long-term mechanical stimulation on chondrocyte-polymer constructs, *Cell Tissue Res.* 331 (2) (2008) 473–483.
- [19] S. Grad, C.R. Lee, K. Gorna, S. Gogolewski, M.A. Wimmer, M. Alini, Surface motion upregulates superficial zone protein and hyaluronan production in chondrocyte-seeded three-dimensional scaffolds, *Tissue Eng.* 11 (1–2) (2005) 249–256.
- [20] S. Grad, S. Gogolewski, M. Alini, M.A. Wimmer, Effects of simple and complex motion patterns on gene expression of chondrocytes seeded in 3D scaffolds, *Tissue Eng.* 12 (11) (2006) 3171–3179.
- [21] Z. Li, S.J. Yao, M. Alini, M.J. Stoddart, Chondrogenesis of human bone marrow mesenchymal stem cells in fibrin-polyurethane composites is modulated by frequency and amplitude of dynamic compression and shear stress, *Tissue Eng. Part A* 16 (2) (2010) 575–584.
- [22] O.F.W. Gardner, N. Fahy, M. Alini, M.J. Stoddart, Joint mimicking mechanical load activates TGFβ1 in fibrin-poly(ester-urethane) scaffolds seeded with mesenchymal stem cells, *J. Tissue Eng. Regen. Med.* 11 (9) (2017) 2663–2666.
- [23] O.F.W. Gardner, G. Musumeci, A.J. Neumann, D. Eglin, C.W. Archer, M. Alini, M.J. Stoddart, Asymmetrical seeding of MSCs into fibrin-poly(ester-urethane) scaffolds and its effect on mechanically induced chondrogenesis, *J. Tissue Eng. Regen. Med.* 11 (10) (2017) 2912–2921.
- [24] A.R. Armiento, M.J. Stoddart, M. Alini, D. Eglin, Biomaterials for articular cartilage tissue engineering: learning from biology, *Acta Biomater.* 65 (2018) 1–20.
- [25] M.L. de Vries-van Melle, E.W. Mandl, N. Kops, W.J. Koevoet, J.A. Verhaar, G.J. van Osch, An osteochondral culture model to study mechanisms involved in articular cartilage repair, *Tissue Eng. Part C Methods* 18 (1) (2012) 45–53.
- [26] F. Shapiro, S. Koide, M.J. Glimcher, Cell origin and differentiation in the repair of full-thickness defects of articular cartilage, *J. Bone Joint Surgery Am.* 75 (4) (1993) 532–553.
- [27] S. Miot, W. Brehm, S. Dickinson, T. Sims, A. Wixmerten, C. Longinotti, A.P. Hollander, P. Mainil-Varlet, I. Martin, Influence of in vitro maturation of engineered cartilage on the outcome of osteochondral repair in a goat model, *Eur. Cells Mater.* 23 (2012) 222–236.
- [28] I.M. Khan, S.J. Gilbert, S.K. Singhrao, V.C. Duance, C.W. Archer, Cartilage integration: evaluation of the reasons for failure of integration during cartilage repair. A review, *Eur. Cells Mater.* 16 (2008) 26–39.
- [29] J.S. Theodoropoulos, J.N. De Croos, S.S. Park, R. Pilliar, R.A. Kandel, Integration of tissue-engineered cartilage with host cartilage: an in vitro model, *Clin. Orthop. Relat. Res.* 469 (10) (2011) 2785–2795.
- [30] M. Peroglio, D. Gaspar, D.I. Zeugolis, M. Alini, Relevance of bioreactors and whole tissue cultures for the translation of new therapies to humans, *Journal of orthopaedic research : official publication of the Orthopaedic Research Society* 36 (1) (2018) 10–21.
- [31] K. Gorna, S. Gogolewski, Biodegradable polyurethanes for implants. II. In vitro degradation and calcification of materials from poly(ε-caprolactone)-poly(ethylene oxide) diols and various chain extenders, *J. Biomed. Mater. Res.* 60 (4) (2002) 592–606.
- [32] K. Gorna, S. Gogolewski, Preparation, degradation, and calcification of biodegradable polyurethane foams for bone graft substitutes, *J. Biomed. Mater. Res. Part A* 67 (3) (2003) 813–827.
- [33] S. Gogolewski, K. Gorna, A.S. Turner, Regeneration of bicortical defects in the iliac crest of estrogen-deficient sheep, using new biodegradable polyurethane bone graft substitutes, *J. Biomed. Mater. Res. Part A* 77 (4) (2006) 802–810.
- [34] G.M. Salzmann, M.S. Buchberger, M.J. Stoddart, S. Grad, S. Milz, P. Niemeyer, N.P. Sudkamp, A.B. Imhoff, M. Alini, Varying regional topology within knee articular chondrocytes under simulated in vivo conditions, *Tissue Eng. Part A* 17 (3–4) (2011) 451–461.
- [35] S. Grad, L. Zhou, S. Gogolewski, M. Alini, Chondrocytes seeded onto poly (L/DL-lactide) 80%/20% porous scaffolds: a biochemical evaluation, *J. Biomed. Mater. Res. Part A* 66 (3) (2003) 571–579.
- [36] C.R. Lee, S. Grad, K. Gorna, S. Gogolewski, A. Goessl, M. Alini, Fibrin-polyurethane composites for articular cartilage tissue engineering: a preliminary analysis, *Tissue Eng.* 11 (9–10) (2005) 1562–1573.
- [37] T. Tschann, I. Hoerler, Y. Houze, K.H. Winterhalter, C. Richter, P. Bruckner, Resting chondrocytes in culture survive without growth factors, but are sensitive to toxic oxygen metabolites, *J. Cell Biol.* 111 (1) (1990) 257–260.
- [38] M.A. Wimmer, S. Grad, T. Kaup, M. Hanni, E. Schneider, S. Gogolewski, M. Alini, Tribology approach to the engineering and study of articular cartilage, *Tissue Eng.* 10 (9–10) (2004) 1436–1445.
- [39] R.L. Trevino, J. Stoia, M.P. Laurent, C.A. Pacione, S. Chubinskaya, M.A. Wimmer, Establishing a live cartilage-on-cartilage interface for tribological testing, *Biotribology (Oxford)* 9 (2017) 1–11.
- [40] M.J. Stoddart, P.I. Furlong, A. Simpson, C.M. Davies, R.G. Richards, A comparison of non-radiative methods for assessing viability in ex vivo cultured cancellous bone: technical note, *Eur. Cells Mater.* 12 (2006) 16–25; discussion 16–25.
- [41] T.D. Schmittgen, K.J. Livak, Analyzing real-time PCR data by the comparative C (T) method, *Nat. Protoc.* 3 (6) (2008) 1101–1108.
- [42] R.W. Farndale, D.J. Buttle, A.J. Barrett, Improved quantitation and discrimination of sulphated glycosaminoglycans by use of dimethylmethylene blue, *BBA* 883 (2) (1986) 173–177.
- [43] R. Iwai, M. Fujiwara, S. Wakitani, M. Takagi, Ex vivo cartilage defect model for the evaluation of cartilage regeneration using mesenchymal stem cells, *J. Biosci. Bioeng.* 111 (3) (2011) 357–364.
- [44] A. Schwab, A. Meeuwse, F. Ehlicke, J. Hansmann, L. Mulder, A. Smits, H. Walles, L. Kock, Ex vivo culture platform for assessment of cartilage repair treatment strategies, *Altex* 34 (2) (2017) 267–277.
- [45] R. Mueller-Rath, K. Gavenis, S. Gravius, S. Andereya, T. Mumme, U. Schneider, In vivo cultivation of human articular chondrocytes in a nude mouse-based contained defect organ culture model, *Bio-Med. Mater. Eng.* 17 (6) (2007) 357–366.
- [46] G.C. Schuller, B. Tichy, Z. Majdisova, T. Jagersberger, M. van Griensven, S. Marlovits, H. Redl, An in vivo mouse model for human cartilage regeneration, *J. Tissue Eng. Regen. Med.* 2 (4) (2008) 202–209.
- [47] M. Jin, E.H. Frank, T.M. Quinn, E.B. Hunziker, A.J. Grodzinsky, Tissue shear deformation stimulates proteoglycan and protein biosynthesis in bovine cartilage explants, *Arch. Biochem. Biophys.* 395 (1) (2001) 41–48.
- [48] M. Jin, G.R. Emkey, P. Siparsky, S.B. Trippel, A.J. Grodzinsky, Combined effects of dynamic tissue shear deformation and insulin-like growth factor I on chondrocyte biosynthesis in cartilage explants, *Arch. Biochem. Biophys.* 414 (2) (2003) 223–231.
- [49] C.C. Wang, N.O. Chahine, C.T. Hung, G.A. Ateshian, Optical determination of anisotropic material properties of bovine articular cartilage in compression, *J. Biomech.* 36 (3) (2003) 339–353.
- [50] R.L. Trevino, C.A. Pacione, A.M. Malfait, S. Chubinskaya, M.A. Wimmer, Development of a Cartilage Shear-Damage Model to Investigate the Impact of Surface Injury on Chondrocytes and Extracellular Matrix Wear, *Cartilage* 8 (4) (2017) 444–455.
- [51] R.J. Custers, W.J. Dhert, D.B. Saris, A.J. Verbout, M.H. van Rijen, S.C. Mastbergen, F.P. Lefeber, L.B. Creemers, Cartilage degeneration in the goat knee caused by treating localized cartilage defects with metal implants, *Osteoarthritis Cartilage* 18 (3) (2010) 377–388.
- [52] R.J. Custers, D.B. Saris, L.B. Creemers, A.J. Verbout, M.H. van Rijen, S.C. Mastbergen, F.P. Lefeber, W.J. Dhert, Replacement of the medial tibial plateau by a metallic implant in a goat model, *J. Orthopaedic Res. Official Publ. Orthopaedic Res. Soc.* 28 (4) (2010) 429–435.
- [53] S.R. Oungoulian, K.M. Durney, B.K. Jones, C.S. Ahmad, C.T. Hung, G.A. Ateshian, Wear and damage of articular cartilage with friction against orthopedic implant materials, *J. Biomech.* 48 (10) (2015) 1957–1964.
- [54] S.N. Redman, G.P. Dowthwaite, B.M. Thomson, C.W. Archer, The cellular responses of articular cartilage to sharp and blunt trauma, *Osteoarthritis Cartilage* 12 (2) (2004) 106–116.
- [55] D.A. Houston, A.K. Amin, T.O. White, I.D. Smith, A.C. Hall, Chondrocyte death after drilling and articular screw insertion in a bovine model, *Osteoarthritis Cartilage* 21 (5) (2013) 721–729.
- [56] W.C. Hembree, B.D. Ward, B.D. Furman, R.D. Zura, L.A. Nichols, F. Guilak, S.A. Olson, Viability and apoptosis of human chondrocytes in osteochondral fragments following joint trauma, *J. Bone Joint Surgery British* 89 (10) (2007) 1388–1395.
- [57] A.J. McGregor, B.G. Amsden, S.D. Waldman, Chondrocyte repopulation of the zone of death induced by osteochondral harvest, *Osteoarthritis Cartilage* 19 (2) (2011) 242–248.
- [58] R.L. Smith, D.R. Carter, D.J. Schurman, Pressure and shear differentially alter human articular chondrocyte metabolism: a review, *Clin. Orthopaedics Related Res.* 427 Suppl (2004) S89–S95.
- [59] M.A. Wimmer, M. Alini, S. Grad, The effect of sliding velocity on chondrocytes activity in 3D scaffolds, *J. Biomech.* 42 (4) (2009) 424–429.
- [60] H. Sadeghi, D.E.T. Shepherd, D.M. Espino, Effect of the variation of loading frequency on surface failure of bovine articular cartilage, *Osteoarthritis Cartilage* 23 (12) (2015) 2252–2258.
- [61] H. Zahedmanesh, M. Stoddart, P. Lezuo, C. Forkmann, M.A. Wimmer, M. Alini, H. Van Oosterwyck, Deciphering mechanical regulation of chondrogenesis in fibrin-polyurethane composite scaffolds enriched with human mesenchymal stem cells: a dual computational and experimental approach, *Tissue Eng. Part A* 20 (7–8) (2014) 1197–1212.
- [62] B.D. Elder, K.A. Athanasiou, Hydrostatic pressure in articular cartilage tissue engineering: from chondrocytes to tissue regeneration, *Tissue Eng. Part B Rev.* 15 (1) (2009) 43–53.
- [63] I. Martin, M. Jakob, D. Schafer, W. Dick, G. Spagnoli, M. Heberer, Quantitative analysis of gene expression in human articular cartilage from normal and osteoarthritic joints, *Osteoarthritis Cartilage* 9 (2) (2001) 112–118.
- [64] A. Cochis, S. Grad, M.J. Stoddart, S. Farè, L. Altomare, B. Azzimonti, M. Alini, L. Rimondini, Bioreactor mechanically guided 3D mesenchymal stem cell chondrogenesis using a biocompatible novel thermo-reversible methylcellulose-based hydrogel, *Sci. Rep.* 7 (2017) 45018.
- [65] S.L. Vega, M.Y. Kwon, K.H. Song, C. Wang, R.L. Mauck, L. Han, J.A. Burdick, Combinatorial hydrogels with biochemical gradients for screening 3D cellular microenvironments, *Nat. Commun.* 9 (1) (2018) 614.
- [66] D.A. Wang, S. Varghese, B. Sharma, I. Strehin, S. Fermanian, J. Gorham, D.H. Fairbrother, B. Cascio, J.H. Elisseeff, Multifunctional chondroitin sulphate for cartilage tissue-biomaterial integration, *Nat. Mater.* 6 (5) (2007) 385–392.
- [67] T.C. Lee, D. Taylor, Bone remodelling: should we cry Wolff?, *Ir. J. Med. Sci.* 168 (2) (1999) 102–105.

- [68] H. Duncan, J. Jundt, J.M. Riddle, W. Pitchford, T. Christopherson, The tibial subchondral plate. A scanning electron microscopic study, *J. Bone Joint Surg. Am.* 69 (8) (1987) 1212–1220.
- [69] T.J. Lyons, S.F. McClure, R.W. Stoddart, J. McClure, The normal human chondro-osseous junctional region: evidence for contact of uncalcified cartilage with subchondral bone and marrow spaces, *BMC Musculoskeletal Disorders* 7 (2006) 52.
- [70] H. Imhof, I. Sulzbacher, S. Grampp, C. Czerny, S. Youssefzadeh, F. Kainberger, Subchondral bone and cartilage disease: a rediscovered functional unit, *Invest. Radiol.* 35 (10) (2000) 581–588.
- [71] Y. Wu, M.J. Stoddart, K. Wuertz-Kozak, S. Grad, M. Alini, S.J. Ferguson, Hyaluronan supplementation as a mechanical regulator of cartilage tissue development under joint-kinematic-mimicking loading, *J. R. Soc. Interface* 14 (133) (2017).
- [72] G.I. Im, Endogenous Cartilage Repair by Recruitment of Stem Cells, *Tissue Eng. Part B Rev.* 22 (2) (2016) 160–171.
- [73] N. Mitchell, N. Shepard, The resurfacing of adult rabbit articular cartilage by multiple perforations through the subchondral bone, *J. Bone Joint Surgery Am.* 58 (2) (1976) 230–233.
- [74] G. Hulsart-Billstrom, J.I. Dawson, S. Hofmann, R. Muller, M.J. Stoddart, M. Alini, H. Redl, A. El Haj, R. Brown, V. Salih, J. Hilborn, S. Larsson, R.O. Oreffo, A surprisingly poor correlation between in vitro and in vivo testing of biomaterials for bone regeneration: results of a multicentre analysis, *Eur. Cells Mater.* 31 (2016) 312–322.
- [75] M.B. Goldring, M. Otero, Inflammation in osteoarthritis, *Curr. Opin. Rheumatol.* 23 (5) (2011) 471–478.
- [76] S.A. Lietman, S. Miyamoto, P.R. Brown, N. Inoue, A.H. Reddi, The temporal sequence of spontaneous repair of osteochondral defects in the knees of rabbits is dependent on the geometry of the defect, *J. Bone Joint Surgery British* 84 (4) (2002) 600–606.